Julie C. Angel, Daniel O. Nelson, and Samuel V. Panno - Comparison of a new GIS-based technique and a manual method for determining sinkhole density: An example from Illinois' sinkhole plain. *Journal of Cave and Karst Studies,* v. 66, no. 1, p. 9-17.

COMPARISON OF A NEW GIS-BASED TECHNIQUE AND A MANUAL METHOD FOR DETERMINING SINKHOLE DENSITY: AN EXAMPLE FROM ILLINOIS' SINKHOLE PLAIN

JULIE C. ANGEL, DANIEL O. NELSON, AND SAMUEL V. PANNO
Illinois State Geological Survey, Natural Resources Building, 615 E. Peabody Dr., Champaign, IL 61820-6964 USA

A new Geographic Information System (GIS) method was developed as an alternative to the hand-counting of sinkholes on topographic maps for density and distribution studies. Sinkhole counts were prepared by hand and compared to those generated from USGS DLG data using ArcView 3.2 and the ArcInfo Workstation component of ArcGIS 8.1 software. The study area for this investigation, chosen for its great density of sinkholes, included the 42 public land survey sections that reside entirely within the Renault Quadrangle in southwestern Illinois.

Differences between the sinkhole counts derived from the two methods for the Renault Quadrangle study area were negligible. Although the initial development and refinement of the GIS method required considerably more time than counting sinkholes by hand, the flexibility of the GIS method is expected to provide significant long-term benefits and time savings when mapping larger areas and expanding research efforts.

Sinkholes, the most diagnostic surface expression of karst landscapes, can be found extensively throughout the world. Approximately 7-10% of the earth's surface has been classified as karst terrane, and more than 25% of the world's population obtains its water supply from karst aquifers (Ford & Williams 1992). Sinkholes provide direct routes for surface water to drain into the underlying karst aquifer. This rapid drainage allows little time for the natural filtration and biodegradation processes that naturally occur in non-karst areas (White 1988). The result is contamination of groundwater resources with bacteria from human and animal sources (Panno *et al*. 1997a; 2003), agrichemicals from row crop production (Waite & Thomson 1993; Panno *et al*. 2003), as well as chemicals that have been spilled or dumped on the surface (Waite &Thomson 1993). Sinkholes also present potential hazards for land use, contributing to soil collapse and erosion by conveying soil underground (Hyatt & Jacobs 1996). Existing and future structures such as commercial and residential developments, transportation infrastructures, and waste disposal sites in karst terranes are at risk for damage from subsidence. Sinkhole density maps depicting the number of sinkholes per unit area provide useful information for determining areas of greatest risk for karst-related groundwater contamination and subsidence.

Sinkhole density maps can be used as a precursor to dye-tracing studies to identify groundwater flow paths and to locate the boundaries of groundwater basins. Panno and Weibel (1999) showed that mapping of sinkhole distribution, sinkhole density, and sinkhole area yielded an approximation of groundwater basin boundaries within the sinkhole plain of southwestern Illinois. Subsequent dye-tracing experiments in this area by Aley *et al*. (2000) used these preliminary maps as a basis for the selection of dye injection points.

Our work is based on sinkholes identified on a 1:24,000 USGS topographic map of the Renault Quadrangle with a contour interval of 20 feet. Applegate (2003) found more sinkholes during karst field observations in the Mt Airy Forest of Hamilton County, Ohio than were indicated on 1:24,000 USGS maps of that area. The study found that sinkhole recognition on contour maps is limited by sinkhole size, map scale, contour interval, and slope.

Gathering and analyzing sinkhole data for sinkhole density studies in mature karst regions has historically required the tedious, time-consuming process of manually counting sinkholes shown on topographic maps. In areas containing thousands to tens of thousands of sinkholes, this manual method requires a significant amount of time, and the patience for careful visual scanning of paper maps to avoid miscounting of sinkholes. We devised a GIS-based method to provide an alternative to hand-counting sinkholes as well as additional applications for karst research and management (e.g., by comparing sinkhole layers with geologic and infrastructure layers). GIS technology provides the means for analyzing the spatial distribution of geographic information, modeling its interactions, and finding patterns and relationships in the data that may be overlooked by previously-used techniques (Szukalski 2002).

SOUTHWESTERN ILLINOIS' SINKHOLE PLAIN

The sinkhole plain, which covers parts of three counties in southwestern Illinois (Fig. 1), contains over 10,000 sinkholes and numerous caves and springs (Panno *et al*. 1997b). The Renault Quadrangle was chosen for this investigation because of its particularly high density of sinkholes (Fig. 2). The study area is on the southwestern flank of the Illinois Basin where Mississippian-age rocks crop out and subcrop under thin

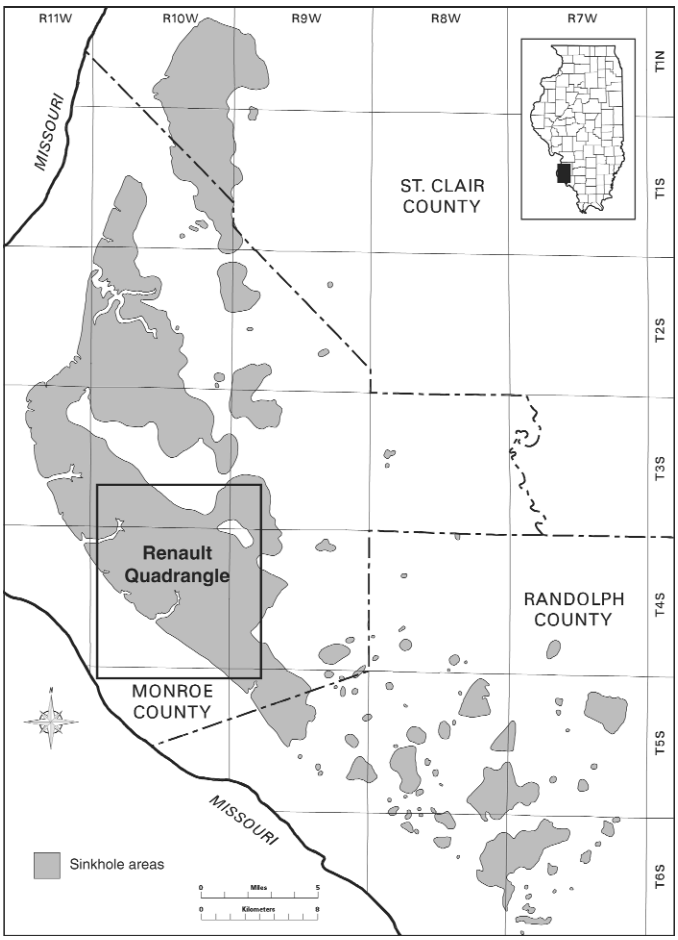

Figure 1. Map showing the location of the Renault Quadrangle within the karst terrane of the southwestern Illinois sinkhole plain, modified from Panno *et al*. (2001)

Figure 2. Aerial view of a typical area within the southwestern Illinois sinkhole plain adjacent to the bluffs of the Mississippi River looking west. Sinkholes are marked by depressions, tree clusters, and ponds. Photograph by Joel Dexter, ISGS, 2000.

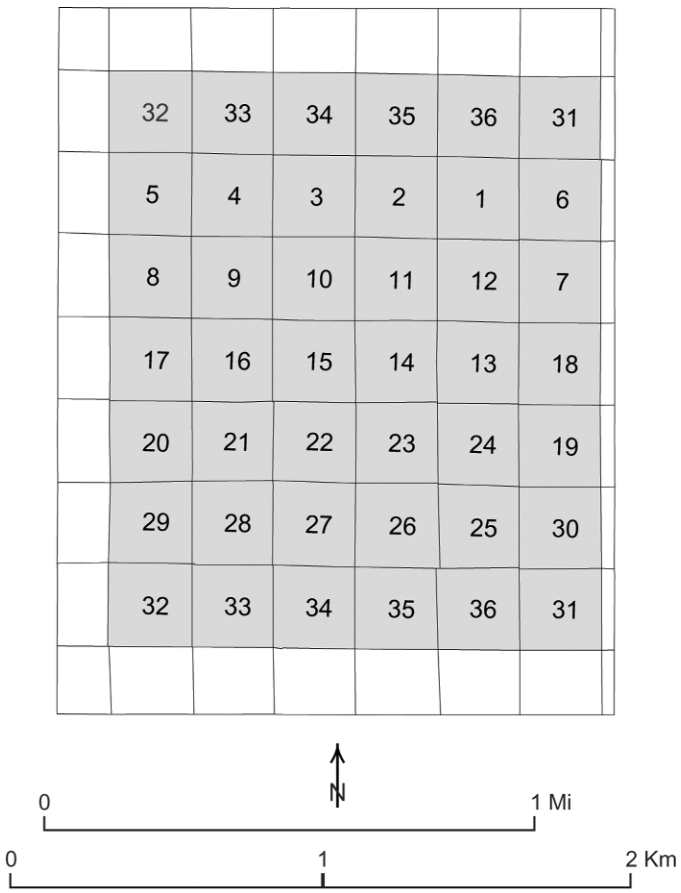

Figure 3. Map of the Renault Quadrangle showing the 42 public land survey sections. Only whole sections (shaded gray, with section number) were included in the study area.

glacial drift and wind-blown loess (Panno *et al*. in press). The main karst-forming formation that underlies much of the sinkhole plain and the Renault Quadrangle is the St. Louis Limestone (Willman *et al*. 1975).

The population of Monroe County, where the Renault Quadrangle is located, has grown by 23.2% from 1990 to 2000 (U.S. Census Bureau 2000). This rapid growth is largely due to urban expansion from the St. Louis metropolitan area. The high degree of karstification, combined with the rapid increase in population, presents many challenges for public officials in protecting groundwater resources and emphasizes the need for sinkhole density and distribution studies to aid in community planning and development.

METHODS

We used ArcView 3.2 and the ArcInfo Workstation component of ArcGIS 8.1 software to create a new GIS-based method that provides an alternative to the hand-counting of sinkholes for density and distribution studies. Sinkhole counts prepared by hand from the printed quadrangle map were compared to

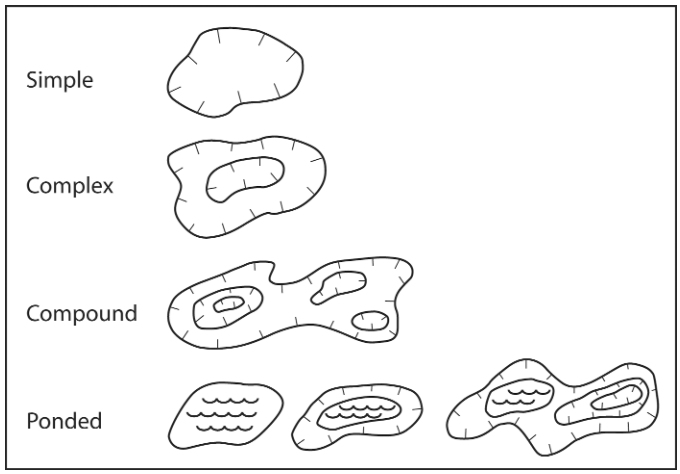

Figure 4. Examples of the four common sinkhole forms in the study area: simple sinkhole – defined by a single, non-nested depression contour; complex sinkhole – defined by one set of nested contours; compound sinkhole – defined by multiple nested depression contours; and ponded sinkholes which can appear as a water body without a depression contour, as ponded water within a simple sinkhole, or as a water body within a compound or complex sinkhole (example shown is within a compound sinkhole). Modified from White, 1988.

those generated by the GIS-based method from USGS Digital Line Graphs (DLGs) of the Renault Quadrangle. GIS methods have previously been used to produce karst maps, to analyze sinkhole density for karst evolution studies (Denizman & Randazzo 2000), for water resource protection (Waite & Thomson 1993), and for inventorying karst features to provide land-use planners and municipalities with data needed for decision making (Kochanov 1999; Brezinski & Dunne 2001; Green *et al*. 2002). Although these studies utilized GIS software, none examined the differences and potential errors that may be involved in using GIS-based techniques to obtain sinkhole counts for density and distribution studies. This investigation examines the possible differences and discrepancies through direct comparison of sinkhole counts obtained from GIS methods with counts obtained from standard manual methods.

The study area used in this investigation included 42 public land survey sections that reside entirely within the Renault Quadrangle of southwestern Illinois (Fig. 3). The partial sections that intersect the quadrangle perimeter were omitted to eliminate the complexities of accounting for incomplete sinkhole counts in these sections.

CLASSIFICATION AND DEFINITION OF SINKHOLE FEATURES

Sinkhole morphology in the Renault Quadrangle is varied, resulting in the need to classify and define those features to be considered for sinkhole counts. Four common types of sinkholes are present in this region: simple, complex, compound, and ponded sinkholes (Fig. 4). Simple sinkholes are defined as having a single, non-nested depression contour, whereas complex sinkholes appear as simple sinkholes, but have two or more nested depression contours. Compound sinkholes are defined as large, irregularly-shaped depression contours with two or more sets of nested depression contours. Ponds that do not appear to be man-made are defined as sinkholes; these circular or elliptical bodies are generally soil-and debris-plugged depressions that retain water. Ponded sinkholes appear as a body of water without a depression contour, as ponded water within a simple sinkhole, or as a water body within a complex or compound sinkhole.

HAND-COUNTING SINKHOLES BY WHOLE SECTION

Sinkholes were counted by hand for each whole section and summed to the nearest quarter sinkhole using a printed copy of the 7.5-minute, 1:24,000-scale, U.S. Geological Survey (USGS) map of the Renault Quadrangle, Monroe County, IL (USGS 1993a). Sinkhole counts were compiled by summing the number of simple and ponded sinkholes, and each of the innermost depression contours within the complex and compound sinkholes (Fig. 5).

Section 4 of the Renault Quadrangle study area (Fig. 6) exemplifies the varied sinkhole features that were considered when generating sinkhole counts. The southwest quarter of the section includes several simple sinkholes, ponded sinkholes, and a man-made pond. The large sinkhole in the center of the southeast quarter is an example of a compound sinkhole, displaying four distinct innermost depression contours, yielding a count of four individual sinkholes. A large complex sinkhole can be seen just below the section label. Several sinkholes can be seen overlapping the southern section line of Figure 6, demonstrating the need for a consistent method of counting sinkholes that overlap section boundaries. During hand-counting, each overlapping sinkhole was apportioned to multiple sections by estimating, to the nearest quarter, the area of the sinkhole within a given section. The partial sinkhole counts added 3.25 sinkholes to the 63 complete sinkholes fully contained within the section, yielding a section count of 66.25 sinkholes.

Each sinkhole was highlighted as it was counted to ensure that each was counted only once. This procedure was followed for each complete section in the Renault Quadrangle. Several sections in the study area had incomplete section lines. These were sketched in by hand to delineate each section and to assign sinkhole counts to the appropriate section. The missing section lines were the result of French colonization land grants and old Indian treaty boundaries that were honored upon establishment of the newer township and range system (Cote 1972). Partial sections along the boundaries of the quadrangle map were not included in this study to eliminate the complexities of accounting for incomplete sinkhole counts in the affected sections.

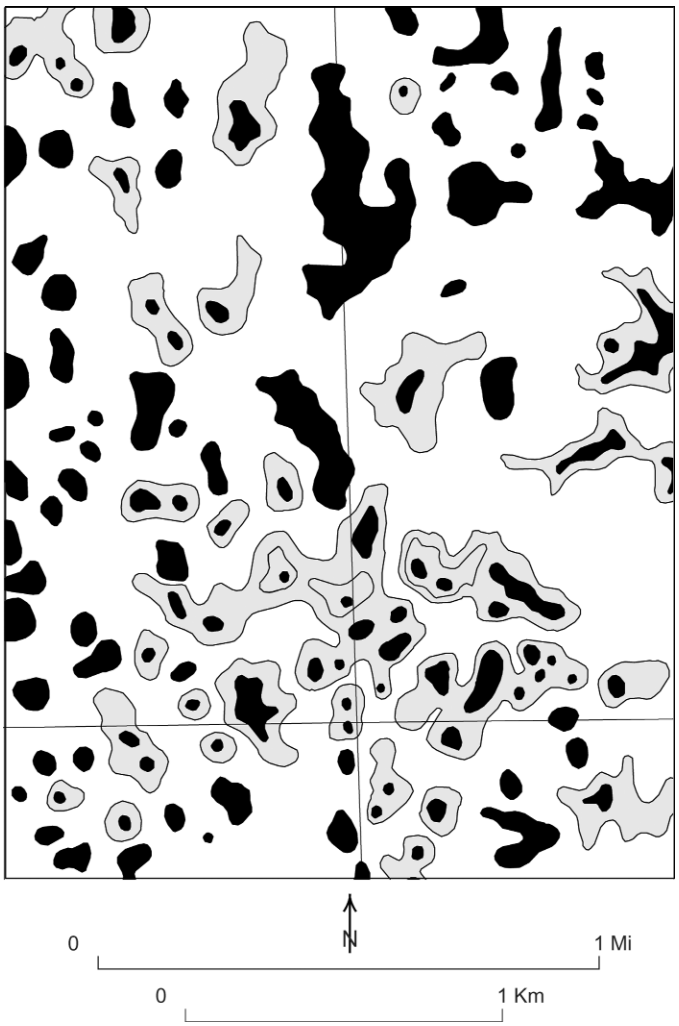

Figure 5. Map of a representative section of the Renault Quadrangle demonstrating what were considered sinkholes for this study. Areas in gray represent complex and compound sinkholes. Areas in black represent either simple sinkholes, ponded sinkholes, or the interior of the innermost depression contours of the complex and compound sinkholes. Each black area was counted as one sinkhole.

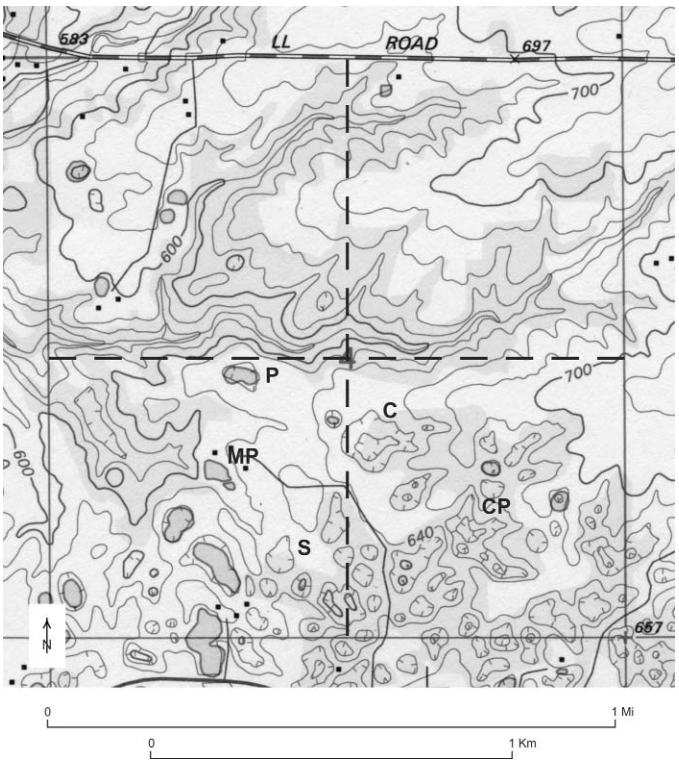

Figure 6. Section 4 of the Renault Quadrangle showing the variety of sinkhole features considered for hand counting. Examples of simple and ponded sinkholes appear in the southwest quarter section. A large compound sinkhole appears just below the center of the southeast quarter section. An example of a complex sinkhole can be seen just below the section label. S=simple, C=complex, CP=compound, P=sinkhole pond, MP=man-made pond. Modified from USGS topographic map of Renault Quadrangle, 1993.

COMPUTER-GENERATED SINKHOLE COUNTS BY SECTION

To derive computer-generated sinkhole counts and related statistics by section, an ArcView project was developed using ArcView 3.2 and the ArcInfo Workstation component of ArcGIS 8.1. The sinkhole data layer was generated for the Renault Quadrangle by combining the Digital Line Graph (DLG) hypsography and hydrography data layers with an Illinois Public Land Survey System (PLSS) data layer. All data were cast on the Universal Transverse Mercator (UTM) coordinate system, zone 15, and the North American Datum of 1983 (NAD83).

The hypsography DLG layer was obtained from the U.S. Geological Survey (1993b) and converted to the ArcInfo coverage format. Depression contours in the coverage were selected as those having DLG codes of major = 20 and minor = 611. A new field named "depression" was added to the coverage and the selected set was assigned a value of depression = 1, indicating that they were indeed depression contours. All other records were assigned a value of depression = 0, indicating that they were non-depression contours.

It was important to ensure that all depression contours represented fully closed polygons. The ArcEdit module of ArcInfo was used to check for any dangling nodes indicating depression contours that did not form closed polygons. Affected polygons were repaired by digitizing the missing portions of the polygons.

Depression polygons were identified in ArcView by using arcs previously labeled as depression boundaries. This was accomplished by using the non-depression contours to identify all non-depression areas, then switching the selection to select all depression areas. This counter-intuitive algorithm is based on the premise that a non-depression contour (e.g. line feature) can almost never be part of the perimeter of a depres-

sion area (e.g. polygon feature). Therefore, every polygon perimeter that is formed, at least in part, by a non-depression contour, must be a non-depression polygon. Switching the selection yields all areas that are depressions. A procedural step was included to check for any non-depression contours that might be imbedded in a depression, such as might occur if a small local high were found within a larger depression. None were expected and none were found to exist.

The Renault Quadrangle hydrography DLG layer (USGS 1993c) was added to identify additional water-filled depression features that were not present in the hypsography layer due to the 20-foot contour interval. A hydrography polygon coverage was prepared using the same methods as for the hypsography layer and a hydrography polygon theme was added to the database. This theme was constrained to only those polygons identified as water bodies (major value = 50), and a depression column was added to the theme's attribute table. Therefore, water bodies in the hydrography data set that were already accounted for in the hypsography data set were automatically removed from consideration. The remaining water bodies were assigned a hydrography depression value = 1. The subset was visually inspected to remove any hydrography features that were not formed by karst processes. These included man-made ponds, lakes or reservoirs, as well as any non-karst depressions present in the Mississippi River flood plain. These non-karst features were assigned a value of depression = 0.

At this point, the database contained the hypsography and hydrography data sets, each with a defined set of unique depressions. A source field was added to each of the two attribute tables as a means of identifying the source DLG for each depression record. A union was executed in ArcInfo to combine the two data sets into a single coverage that contained all depression polygons. After the coverage was built, polygon topology was verified and the coverage was checked for any label or node errors. The sinkhole attribute table was inspected to verify that polygon attributes were as expected, confirming that all polygons were labeled as depression = 1 and that each record contained a source column entry.

The next several procedures were perhaps the most important steps in the development of the method. In the hand-counting method, sinkhole counts were compiled by counting the number of simple and ponded sinkholes, as well as the innermost depression contours of complex and compound sinkholes. The first step to derive similar counts using GIS methods was to identify the singular, complex, and compound depression polygons within the sinkhole data layer. This was accomplished in ArcInfo by merging all nested polygons in the sinkholes coverage and creating a new coverage called "compound" that contained all outer boundaries of the compound and complex depressions plus the simple and ponded depression polygons. The compound arcs feature class was added to the ArcView project and used to select all adjacent depression polygons. This produced the set of depression polygons that included all the outer polygonal rings of the complex and compound depression polygons, and all the simple and ponded

Goal

Populate a data field called "interior" which indicates the nesting level values for all nested polygons in a complex or compound depression and identifies the polygons that participate in a complex or compound sinkhole.

Assumptions and constraints

- A set of nested polygons may have 1 to many nesting levels.
- The series (0 to n) for any set of nested polygons is an uninterrupted, continuous sequence of positive integers that increment by 1.
- Non-nested polygons and the outermost polygon of the complex and compound depressions will have nesting values of zero.
- The remaining polygons have an initial interior value of interior = 1.

Algorithm

- Set n equal to the initial interior value assigned to all the components of the nested polygons in the data set (n=1)
- Start Loop: For each value of n, from n to maximum nested level, by increments of +1, do the following:
  - In ArcInfo:
    - Dissolve sinkholes interior<n> interior poly
    - Build interior<n> line
  - In ArcView:
    - Add interior<n> arcs to view
    - Select interior<n> arcs
    - Select polygons from sinkholes theme adjacent to the selected set
    - Open sinkholes table and switch selection
    - Select from set, interior > 0
    - Calculate selected set to interior = n + 1
    - Save/Close ArcView
  - Increment n (i.e. n = n + 1)
- Loop
- Select sinkhole theme polygons with interior <> 0
- Select features of active theme that intersect selected sinkholes features
- Calculate comp = 1

[End]

Figure 7. Selection algorithm A for determining the interior nesting levels of all complex and compound polygons within sinkhole areas.

polygons. By switching the selection, all polygons that represented the interior components of the complex and compound depression were isolated. A field named "comp" was added, and all interior components of the complex and compound depressions were assigned a comp value = 1. A field named "interior" was added, and all interior components of the selected set were assigned a value of interior = 1 to identify them as part of a complex or compound sinkhole.

It was necessary to determine the interior nesting levels of the complex and compound depressions to ultimately identify the innermost depression polygons to be counted as sinkholes. Complex and compound depressions could contain several sets of nested polygons, making it possible for these nested depressions to have several innermost polygons. Interior nesting levels were determined using algorithm A (Fig. 7). The result was that each complex or compound depression had a series of nested pseudo-concentric rings. The rings were labeled in

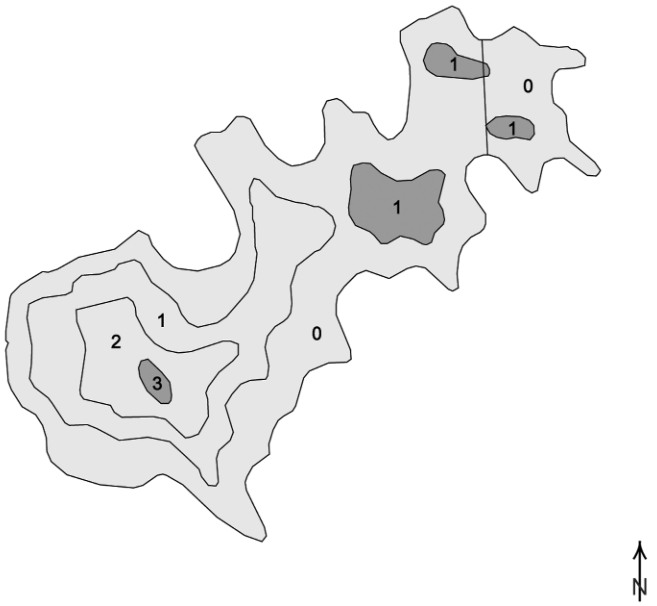

Figure 8. Compound sinkhole with labeled nesting levels. Outermost nested polygon is labeled 0. Innermost is labeled 3. The four darker polygons, one labeled 3 and three labeled 1, were counted as sinkholes as each is locally innermost. Note also the section line that divides the northeast lobe. The uppermost interior polygon is apportioned between two sections.

ascending order where zero was the outermost ring and "n", with a maximum value of three (Fig. 8), was the innermost.

Singular depressions were defined as simple and ponded depressions, and the innermost polygons of any complex or compound depression. Identifying these singular depressions in ArcView produced the set from which sinkhole counts were ultimately derived. Algorithm B (Fig. 9) illustrates the singular depression selection process.

Unique ID values were assigned to each polygon in the sinkhole attribute table. To identify the nested polygon components of any complex or compound polygon set, compound IDs were assigned to each set by first transferring the unique IDs of any complex or compound component to the compound coverage, then spatially joining the sinkhole and compound coverages. This join enabled the transfer of all complex and compound IDs to the interior nested polygons, providing a means for identifying all the components of any complex or compound sinkhole, either as an individual polygon or as a component of the compound group. This completed the generation of a thoroughly attributed sinkhole coverage.

The final step in preparing the data for analysis involved intersecting sinkhole data with township, section, and range data for the quadrangle. Adding township, section, and range parameters to the sinkhole polygon attributes table provided the means to apportion sinkholes divided by section lines into the appropriate sections.

To obtain sinkhole counts per section, it was necessary to

Goal

Populate a data field called "singular" which indicates whether or not a polygon is the innermost of a nested set of polygons, or a simple or ponded polygon. An innermost, simple or ponded polygon will be set to singular= 1, otherwise it will be set to singular= 0.

Assumptions and constraints

- The nesting level values for all polygons have already been determined and assigned to a data field called "interior".
- The outermost polygon of a set of nested polygons has a nesting level value of zero (interior = 0).
- The innermost polygon of a set of nested polygons has a nesting level of n, where n is a positive integer.
- The series (0 to n) for any set of nested polygons is an uninterrupted, continuous sequence of positive integers that increment by 1.
- A set of nested polygons may have 1 to many innermost polygons. For example, a complex sinkhole of large size may have several sets of nested depression polygons contained within the overall area of depression.

Algorithm

- Set n equal to the maximum value of "interior" for the set of all nested polygons in the entire data set.
- Select the set of polygons that have interior = n
- Start Loop: For each value of n, from n to 0, by increments of -1, do the following:
  - Set singular = 1 for the selected set
  - Select a new set of polygons having interior >= n
  - Select the set of polygons adjacent to the selected set
  - Switch the selected set (non-selected become selected and vice versa)
  - Decrement n (i.e., n = n - 1)
  - Reselect from the current set the subset of polygons with interior = n
- Loop
- Clear selected set
- Select comp = 0
- Set singular = 1 for selected set
- Select the set of all polygons that have singular = 1
- Switch the selected set (non-selected become selected and vice versa)
- Set singular = 0 for the selected set

[End]

Figure 9. Selection algorithm B for determining the set of innermost polygons from a set of nested polygons representing elevation contour ranges within sinkhole areas, and the simple and ponded polygons.

obtain a "countable" value for the partial sinkhole components that overlap section lines. This was accomplished by relating the total area of any overlapping sinkhole to the areas of its partial components and deriving a value between 0 and 1. Total area values for individual sinkholes were determined by summing area by unique ID in the sinkhole attribute table. The resulting summary table was joined to the sinkhole attribute table based on the unique ID value. A weighted count for each sinkhole was derived by dividing the area of the partial component by the area of the entire sinkhole. Sinkhole counts per section were finalized by selecting the set of sinkholes having singular = 1 (countable sinkholes), and summing the weighted count by township, section, and range. A total sinkhole count

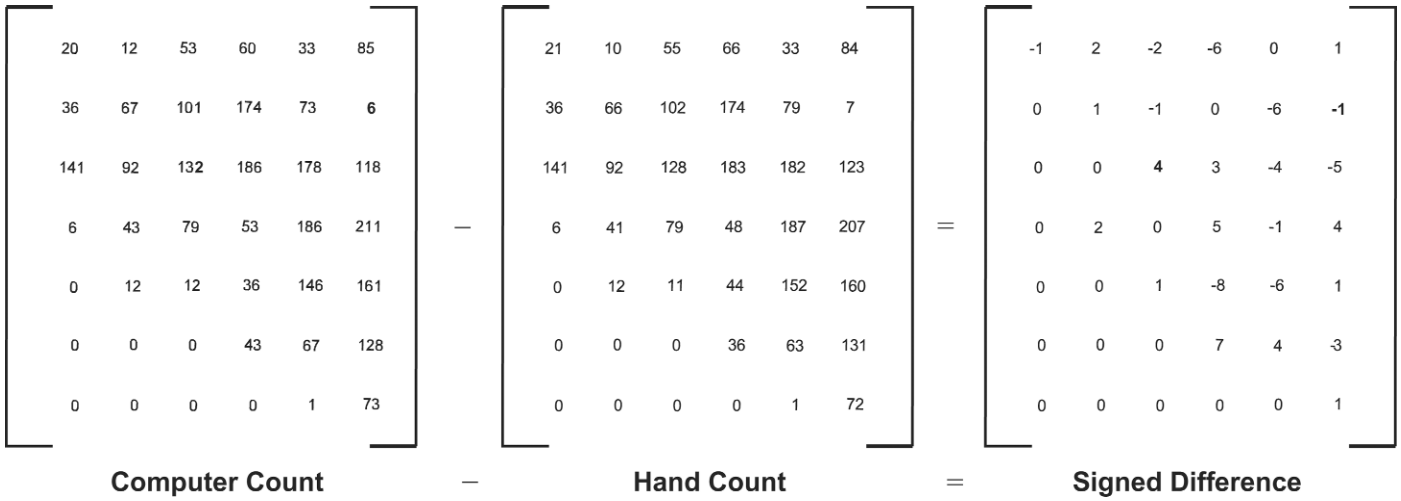

Figure 10. Matrix representation of computer counts minus hand counts and the resulting differences for each section in the study area. Section counts were rounded to the nearest whole number.

for the entire Renault study area was derived by summing all the weighted counts.

ANALYSIS AND COMPARISON OF COUNTING METHODS

Sinkhole counts from the GIS database totaled 2,823 within the study area, while 2,830 sinkholes were counted manually using the paper map, yielding a negligible difference. Although the difference is small, potential sources of error were examined to reveal any shortcomings that may exist in either counting method.

Comparison of the computer- and hand-counts by section (Fig. 10) demonstrated differences that ranged from an over-count of 7 sinkholes to an under-count of 8 sinkholes by the GIS method relative to the hand-counted standard. Sinkholes were over-counted by the GIS method in 13 sections, under-counted in 12 sections, and matched the hand-counts in 12 sections. The remaining 5 sections, which were located completely within the Mississippi River floodplain, contained no sinkholes. The counting errors exhibited at the section level essentially cancelled each other out through summation, resulting in the small difference seen in the total study area counts for the two methods.

The total sinkhole counts for the study area completed by hand and by computer were compared using the Wilcoxon signed-rank test (Snedecor & Cochran 1989); a nonparametric test used as a substitute for the t-test for paired samples. The null hypothesis (the two populations of sinkhole counts are equal) was accepted ($P = 0.95$) on the basis of the test. That is, the results of the two counting methods were found to be statistically equivalent.

Sections with numerical discrepancies were examined in an attempt to determine causes of the disparities. Minor differences in counts for several sections occurred from differences in assigning proportional counts for those sinkholes that overlapped section lines. The GIS method is capable of exactly apportioning sinkholes split by section boundaries, whereas accurate apportionment for anything less than a quarter of a sinkhole is difficult to attain with hand-counting.

The addition of the hydrography data layer added desired ponded sinkholes to the database, however, unwanted man-made bodies of water were added as well. In this area, most man-made ponds can be identified by the appearance of a square edge that represents the dammed side of the pond, and were removed from both the paper map and the GIS database based on the presence of this feature. Identifying the squared sides of a man-made pond proved more difficult using GIS analysis due to the square nature of the digitized vectors that form the polygon boundaries. It was necessary to use the zoom feature to adequately view the smaller ponds, yet zooming tended to accentuate the square nature of the vectors. These difficulties with pond labeling caused several minor errors by removing sinkhole ponds or by failing to remove man-made ponds.

A slight difference in the locations of the missing section lines that were added became evident when comparing the digital- and hand-counts in the southeast quarter of the quadrangle. The absent section lines were added to the statewide digital Public Land Survey System (PLSS) layer when it was developed in the 1980s. The absent lines were drawn on the paper map during hand-counting. The slight locational discrepancies between these two versions of the added section lines would not have been discovered if not for the discrepancy they caused in sinkhole counts. This difference in line placement skewed the actual counts for sections on both sides of the lines, causing over- and under-counts that would not have been present had both lines been placed in the same map location.

Most of the discrepancies in section and overall counts were accounted for within the visual estimation errors of the

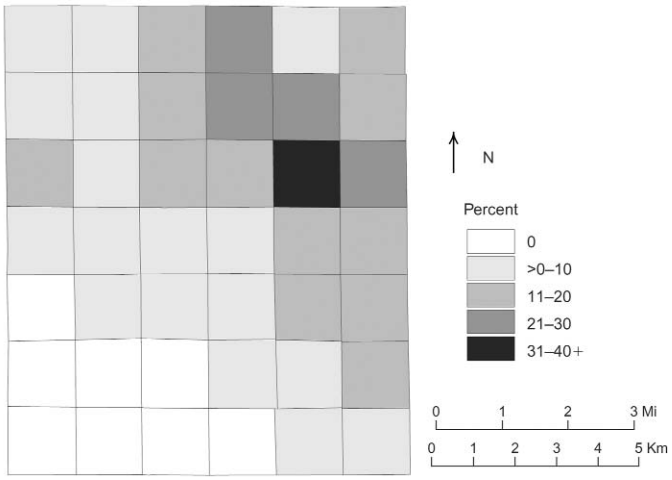

Figure 11. Map produced from the GIS database showing the sinkhole area as a percentage of total area for each section in the study area.

apportionment of sinkholes which overlapped multiple sections, by the "square pond" problem, and by the slight discrepancies of section line locations. Additional sources of error could include errors in the hand-counts, digitizing errors in the original production of the DLG layers, undetected GIS procedural errors, or disparity in data sources. Despite sinkhole count differences present at the section level, the two overall study area counts were virtually identical. Therefore, we concluded that reliable sinkhole counts can be obtained using GIS-based methods.

In addition to producing accurate sinkhole counts, expanded statistical and spatial analyses are possible using GIS techniques. Descriptive statistics and figures can be easily generated for parameters such as sum of sinkhole area per section, sinkhole counts by section, and percent study area in sinkholes. For example, analysis of the percentage of sinkhole area per section (Fig. 11), as well as sinkhole counts per section (Fig. 12), can reveal sinkhole distribution trends that are useful for determining areas of greater risk for karst-related groundwater contamination and subsidence. The sinkhole database prepared in this study was used extensively by Panno *et al*. (in press) to generate a 1:24,000-scale sinkhole map of the Renault 7.5-minute Quadrangle. Digital geospatial data also provide long-term benefits for dynamic karst studies because new themes can be added, old themes deleted, and additional analyses and studies performed as new ideas are developed.

Finally, an examination of the time required to implement both methods revealed that the development and refinement of the GIS methodology for this investigation was approximately three times greater than the time consumed in hand-counting a single quadrangle. This was expected, but not discouraging, as the initial time and effort spent creating the database will facilitate quicker processing and broaden analysis opportunities for the study of additional quadrangles. With an established data-

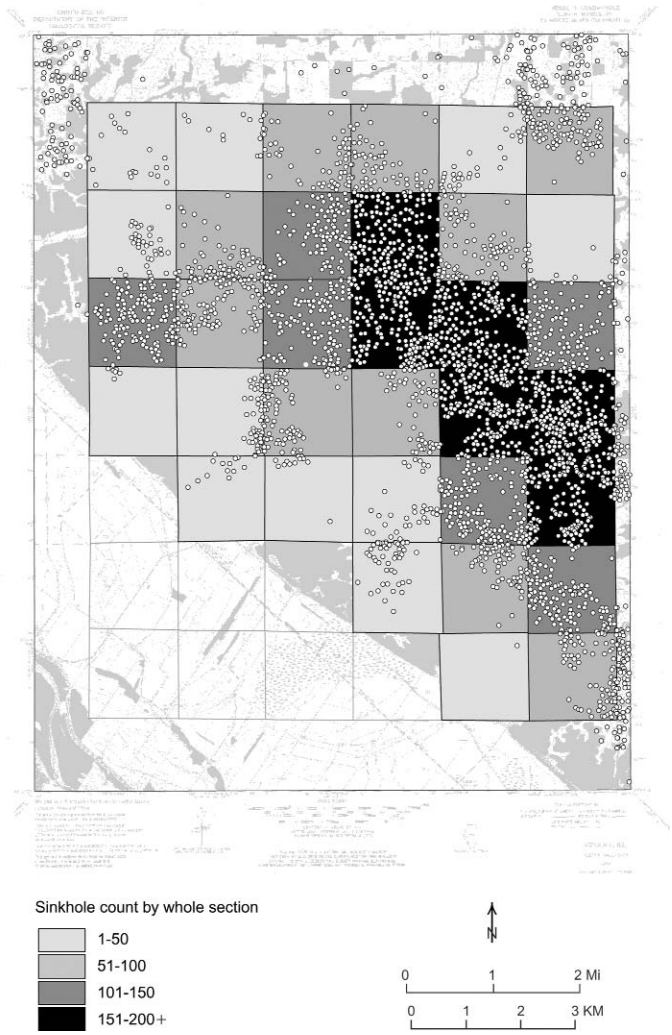

Figure 12. Map produced from the GIS database showing the number of sinkholes for each section in the study area. Map is layered with the Renault Quadrangle DRG, sinkhole count per section, and the sinkhole label points (each label point represents a countable sinkhole).

base in place, we expect that the processing of additional quadrangles with similar sinkhole density would require approximately 6-8 hours. Hand counting a densely populated quadrangle requires approximately 10-12 hours. Significant time savings would be realized when applying the GIS method to an area larger than a single quadrangle (e.g., the entire sinkhole plain). Finally, changes and revisions to GIS-produced maps and statistical data can be easily implemented, whereas changes to paper maps generally require the production of an entirely new, updated map.

CONCLUSION

Density and distribution studies of sinkholes in karst areas provide a means for identifying areas at risk for karst-related groundwater contamination and subsidence. The alternative of manually gathering and analyzing data on sinkhole density and distribution in mature karst terranes is a tedious and time-consuming process.

Differences between the sinkhole counts derived from manual and GIS-based methods for our study area were statistically negligible. The GIS method employed in this investigation yielded accurate sinkhole counts, provided opportunities for broader data analysis, and created a database for future analyses. Although possible to complete by hand, the descriptive statistics and map figure relating to the percentage of sinkhole area per section would require significant time and effort to produce manually. The time required to develop the GIS method was approximately three times greater than the time required to complete the hand-count of sinkholes on the paper quadrangle map. However, once the method and database are in place, additional quadrangles can be processed in about one-half the time required for the manual method.

ACKNOWLEDGEMENTS

The authors thank Edward Mehnert, Beverly Herzog, Robert Krumm, and Jonathan Goodwin for their critical review of this document and for their suggestions that greatly improved the quality of this document. This research was supported by the Illinois State Geological Survey, Illinois Department of Natural Resources. Publication of this article has been authorized by the Chief of the Illinois State Geological Survey.

REFERENCES

Aley, T., Moss, P., & Aley, C., 2000, Delineation of recharge areas for four biologically significant cave systems in Monroe and St. Clair counties, Illinois: Unpublished final report to the Illinois Nature Preserves Commission and the Monroe County Soil and Water Conservation District, 254p.

Applegate, P., 2003, Detection of sinkholes developed on shaly Ordovician limestones, Hamilton County, Ohio, using digital topographic data: dependence of topographic expression of sinkholes on scale, contour interval, and slope: Journal of Cave and Karst Studies, v. 65, n. 2, p. 126-129.

Brezinski, D.K., & Dunne, L.E., 2001, Geographic Information Systems (GIS) applications to karst studies - Frederick Valley, Maryland: [Extended Abstract] *in* Digital Mapping Techniques '01 - Workshop Proceedings, U.S. Geological Survey Open-File Report 01-223, Tuscaloosa, Alabama, May 20-23, 2001, p. 207-208.

Cote, W.E., 1972, Guide to the use of Illinois topographic maps: Illinois State Geological Survey Educational Extension Service Publication (revised 1978), Killey, M.M., DuMontelle, P.B., and Reinertsen, D.L., p. 9.

Denizman, C., & Randazzo, A.F., 2000, Post-Miocene subtropical karst evolution, lower Suwannee River basin, Florida: Geological Society of America Bulletin, v. 112, n. 12, p. 1804-1813.

Ford, D.C., & Williams, P.W., 1992, Karst Geomorphology and Hydrology: New York, Chapman and Hall, 601 p.

Green, J.A., Marken, W.J., Alexander, E.C., & Alexander, S.C., 2002, Karst unit mapping using geographic information system technology, Mower County, Minnesota, USA: Environmental Geology, v. 42, n. 5, p. 457-461.

Hyatt, J.A., & Jacobs, P.M., 1996, Distribution and morphology of sinkholes triggered by flooding following Tropical Storm Alberto at Albany, Georgia, USA: Geomorphology, v. 17, p. 305-316.

Kochanov, W.E., 1999, The integration of sinkhole data and Geographic Information Systems: An application using ArcView 3.1: [Extended Abstract] *in* Digital Mapping Techniques '99 - Workshop proceedings, U.S. Geological Survey Open-File Report, Reston, VA, 1999, p.183.

Panno, S.V., Weibel, C.P., Krapac, I.G., & Storment, E.C., 1997a, Bacterial contamination of groundwater from private septic systems, *in* Proceedings, Sixth Multidisciplinary Conference on Sinkholes and the Engineering and Environmental Impacts of Karst, Springfield, MO, p. 1-7.

Panno, S.V., Weibel, C.P., & Li, W.B., 1997b, Karst regions of Illinois: Illinois State Geological Survey Open File Report, 1997-2, 42 p.

Panno, S.V., & Weibel, C.P., 1999, Delineation and characterization of the groundwater basins of four cave systems of southwestern Illinois' sinkhole plain: [Abstract] *in* Karst Modeling: Symposium Proceedings, A.N. Palmer, M.V. Palmer & I.D. Sasowsky (eds.), Karst Waters Institute Special Publication 5, Charlottesville, VA, p. 244.

Panno, S.V., Hackley, K.C., Hwang, H.H., & Kelly, W.R., 2001, Determination of the sources of nitrate contamination in karst springs using isotopic and chemical indicators: Chemical Geology, v. 179, p. 115.

Panno, S.V., Kelly, W.R., Weibel, C.P., Krapac, I.G., & Sargent, S.L., 2003, Water Quality and Agrichemical Loading in Two Groundwater Basins of Illinois' Sinkhole Plain: Illinois State Geological Survey Environmental Geology Series 156, 36p.

Panno, S.V., Angel, J.C., Nelson, D.O., Weibel, C.P., & Devera, J.A., 2004, Distribution and Density of Sinkholes: Renault 7.5 Minute Quadrangle: Illinois State Geological Survey Quadrangle Series Map, (in press).

Snedecor, G.W., & Cochran, W.G., 1989, Statistical methods: Ames, Iowa State University Press, 503 p.

Szukalski, B.W, 2002, Introduction to cave and karst GIS: Journal of Cave and Karst Studies, Cave and Karst Studies Special Issue, v. 64, n. 1, p. 3.

U.S. Census Bureau, 2000, State and County quickfacts, http://quickfacts.census.gov/qfd/index.html.

U.S. Geological Survey (USGS), 1993a, Renault, IL: U.S. Geological Survey 7.5 minute quadrangle map, 1:24,000 scale, 1 sheet, mapped 1968, revised 1993, Denver, CO.

U.S. Geological Survey (USGS), 1993b, Renault, IL: U.S. Geological Survey hypsography DLG map, 1:24,000 scale, 1 sheet, mapped 1970, revised 1993.

U.S. Geological Survey (USGS), 1993c, Renault, IL: U.S. Geological Survey hydrography DLG map, 1:24,000 scale, 1 sheet, mapped 1970, revised 1993.

Waite, L.A. & Thomson, K.C., 1993, Development, Description, and Application of a Geographic Information System Data Base for Water Resources in Karst Terrane in Greene County, Missouri: Rolla, Missouri, U.S. Geological Survey Water-Resources Investigations Report 93-4154, 31p.

White, W.B., 1988, Geomorphology and Hydrology of Karst Terranes: New York, Oxford University press, 464 p.

Willman, H.B., Atherton, E., Buschbach, T.C., Collinson, C., Frye, J.C., Hopkins, M.E., Lineback, J.A., & Simon, J.A., 1975, Handbook of Illinois Stratigraphy, Urbana, Illinois: Illinois State Geological Survey, Bulletin 95, 261p.